

HET Publication Report

HET Board Meeting

29/30 November 2022

Penn State

Executive Summary

- There are now 486 peer-reviewed HET publications
 - Twenty-nine papers published in 2021
 - As of 21 November, 28 papers published in 2022
- HET papers have 33945 citations
 - Average of 70, median of 35 citations per paper
 - H-number of 97
 - 89 papers have ≥ 100 citations; 195 have ≥ 50 cites
- Wide angle (non-HETDEX) surveys account for 25% of papers and 33% of citations.
- Synoptic (e.g., planet searches) and Target of Opportunity (e.g., supernovae and γ -ray bursts) programs have produced 47% of the papers and 49% of the citations, respectively.
- HETDEX has published sixteen papers.
- LRS2 and HPF have published 41 and 36 papers, respectively.
- Listing of the HET papers (with ADS links) is given at
<http://personal.psu.edu/dps7/hetpapers.html>

HET Program Classification

| Code | Type of Program | Examples |
|------|--------------------|--------------------------------|
| 1 | ToO | Supernovae, Gamma-ray Bursts |
| 2 | Synoptic | Exoplanets, Eclipsing Binaries |
| 3 | One or Two Objects | Halo of NGC 821 |
| 4 | Narrow-angle | HDF, Virgo Cluster |
| 5 | Wide-angle | Blazar Survey |
| 6 | HET Technical | HET Queue |
| 7 | HETDEX | Dark Energy with BAO |
| 8 | Other | HET Optics |

Programs also broken down into “Dark Time”, “Light Time”, and “Other”.

Peer-reviewed Publications

- There are now 486 journal papers that either use HET data or (nine cases) use the HET as the motivation for the paper (e.g., technical papers, theoretical studies).
- Except for 2005, approximately 22 HET papers were published each year since 2002 through the shutdown. A record 44 papers were published in 2012.
- Through 21 November the current year has produced 28 HET papers.
- Each HET partner has published at least 16 papers using HET data.
- Nineteen papers have been published from NOAO time.
- A total of 28 SDSS SNe papers have appeared in print. (The final data release paper appeared in early 2018.)
- A total of 89 publications present data acquired with the new instrumentation (LRS2/HPF/VIRUS).

A listing of the HET papers (with ADS links) is given at
<http://personal.psu.edu/dps7/hetpapers.html>

Citations to Peer-reviewed Publications

- The 33945 HET papers have garnered 32707 citations for an average of 69.9 per paper (median number is 35).
- The HET's H-number is now 97.
- The number of citations ranges from 0 to 1456. Eighteen papers have one or zero citations; 195 have 50 or more citations.
- Approximately 33% of the HET citations are produced by “Wide angle” surveys (non-HETDEX). This category was the primary science program for the “SST”.
- The four most cited Wide Angle Survey (non-HETDEX) papers have 461, 575, 709, and 769 citations.
- “Dark Time” projects have average higher citation rates (86) than “Light Time” programs (50). The roughly 2:1 ratio has been steadily decreasing over time.
- The synoptic programs (primarily planet searches) are a significant component of both the number of publications and citations (top four papers have 270, 278, 313, and 492 citations).
- “Target of Opportunity” impact: Top four ToO papers have 403, 429, 597, and 1456 citations.
- The SDSS Supernova Survey (HET played key role in obtaining spectra of the faintest targets) produced an average of 176 citations per paper, as well as the highest-cited work (1456 citations from 2014 publication).

Summary of HET Publications November 2022

| Year | Papers | Total | Total Citations | Average Citations |
|-------|--------|-------|-----------------|-------------------|
| 2000 | 9 | 9 | 592 | 65.78 |
| 2001 | 13 | 22 | 1394 | 107.23 |
| 2002 | 10 | 32 | 1108 | 110.80 |
| 2003 | 20 | 52 | 1748 | 87.40 |
| 2004 | 21 | 73 | 1637 | 77.95 |
| 2005 | 7 | 80 | 673 | 96.14 |
| 2006 | 21 | 101 | 1849 | 88.05 |
| 2007 | 21 | 122 | 2291 | 109.10 |
| 2008 | 24 | 146 | 3148 | 131.17 |
| 2009 | 26 | 172 | 3158 | 121.46 |
| 2010 | 33 | 205 | 2805 | 85.00 |
| 2011 | 26 | 231 | 2520 | 96.92 |
| 2012 | 44 | 275 | 3540 | 80.45 |
| 2013 | 23 | 298 | 852 | 37.04 |
| 2014 | 24 | 322 | 2710 | 112.92 |
| 2015 | 28 | 350 | 1289 | 46.04 |
| 2016 | 19 | 369 | 862 | 45.37 |
| 2017 | 8 | 377 | 206 | 25.75 |
| 2018 | 9 | 386 | 424 | 47.11 |
| 2019 | 19 | 405 | 366 | 19.26 |
| 2020 | 24 | 429 | 390 | 16.25 |
| 2021 | 29 | 458 | 291 | 10.03 |
| 2022 | 28 | 486 | 92 | 3.29 |
| Total | 486 | | 33945 | 69.85 |

Summary of Program Classes

| Code | Class | Papers | Total Citations | Average Citations |
|------|---------------|--------|-----------------|-------------------|
| 1 | ToO | 89 | 9165 | 102.98 |
| 2 | Synoptic | 139 | 7340 | 52.81 |
| 3 | Single Object | 73 | 3132 | 42.90 |
| 4 | Pencil Beam | 36 | 2479 | 68.86 |
| 5 | Wide Angle | 120 | 11291 | 94.09 |
| 6 | Technical | 11 | 379 | 34.45 |
| 7 | HETDEX | 16 | 139 | 8.69 |
| 8 | Other | 2 | 20 | 10.00 |

Summary of Dark/Light Time

| Code | Time | Papers | Total Citations | Average Citations |
|------|-------|--------|-----------------|-------------------|
| 1 | Dark | 275 | 23603 | 85.83 |
| 2 | Light | 199 | 9964 | 50.07 |
| 3 | Other | 12 | 378 | 31.50 |

HET Publications Sorted by Journal

| Papers | Average Citations | Journal |
|--------|----------------------|---|
| 96 | 70.11 | The Astronomical Journal |
| 198 | 68.33 | The Astrophysical Journal |
| 38 | 55.18 | The Astrophysical Journal (Letters) |
| 13 | 63.31 | The Publications of the A.S.P. |
| 20 | 131.65 | The Astrophysical Journal Supplement Series |
| 11 | 198.45 | Nature |
| 1 | 269.00 | Science |
| 48 | 35.71 | M.N.R.A.S |
| 2 | 33.00 | M.N.R.A.S. (Letters) |
| 48 | 73.00 | Astronomy and Astrophysics |
| 5 | 36.20 | Astronomy and Astrophysics (Letters) |
| 1 | 20.00 | J.C.A.P. |
| 1 | 106.00 | Optics Express |
| 1 | 4.00 | Astronomische Nachrichten |
| 1 | 6.00 | J.A.T.I.S. |
| 1 | 57.00 | Optica |
| 1 | 22.00 | Optics Letters |

HET Publications Sorted by Instrument

| Code | Instrument | Papers | Total Citations | Average Citations |
|------|------------|--------|-----------------|-------------------|
| 1 | None | 7 | 288 | 41.14 |
| 2 | LRS | 228 | 22909 | 100.48 |
| 3 | MRS | 1 | 24 | 24.00 |
| 4 | HRS | 159 | 9502 | 59.76 |
| 5 | UFOE | 2 | 115 | 57.50 |
| 6 | LRS2 | 41 | 538 | 13.12 |
| 7 | HPF | 36 | 478 | 13.28 |
| 8 | VIRUS | 12 | 91 | 7.58 |

“Hot Papers” (2020-2022)

(81) A Giant Planet Candidate Transiting a White Dwarf. Vanderburg, A., et al. 2020, Nature

(45) Evidence for He I 10830 Å Absorption During the Transit of a Warm Neptune. Ninan, J., et al. 2020, ApJ

(44) I Spy transits and Pulsations: Empirical Variability in White Dwarfs Using Gaia and the Zwicky Transient Facility. Guidry, J., et al. 2021, ApJ

(34) A sub-Neptune-sized Planet Transiting the M2.5 Dwarf G-40: Validation with the Habitable-zone Planet Finder. Stefansson, G., et al. 2020, AJ

(28) Kepler-1661 b: A Neptune-sized Kepler Transiting Circumbinary Planet Around a Grazing Eclipsing Binary. Socia, Q.J., et al. 2020, AJ

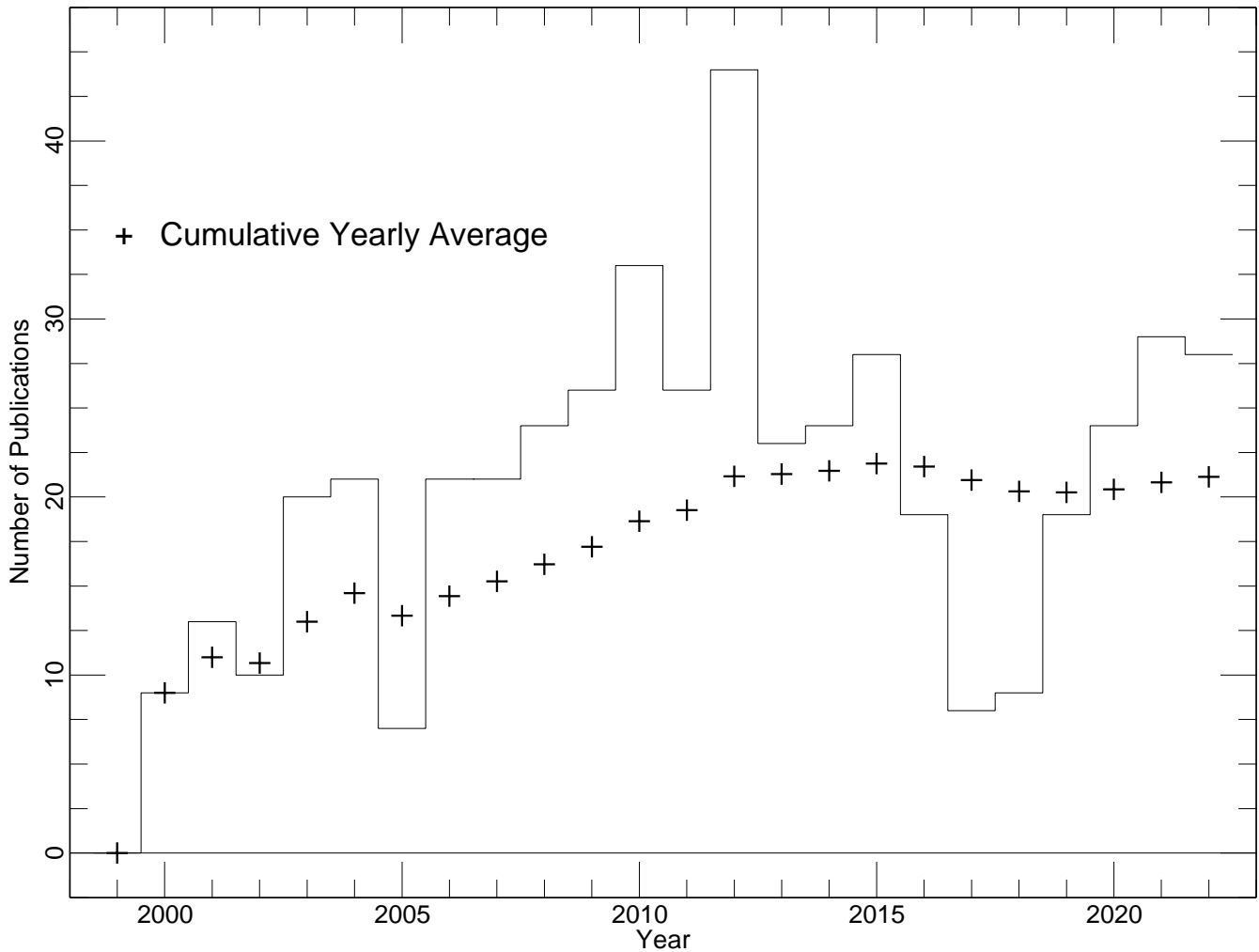
(27) A WC/WO Star Exploding Within an Expanding Carbon-Oxygen-Neon Nebula. Gal-Yam, A., et al. 2022, Nature

(25) The Hobby-Eberly Telescope Dark Energy Experiment (HETDEX) Survey Design, Reductions, and Detections. Gebhardt, K., et al. 2021, ApJ

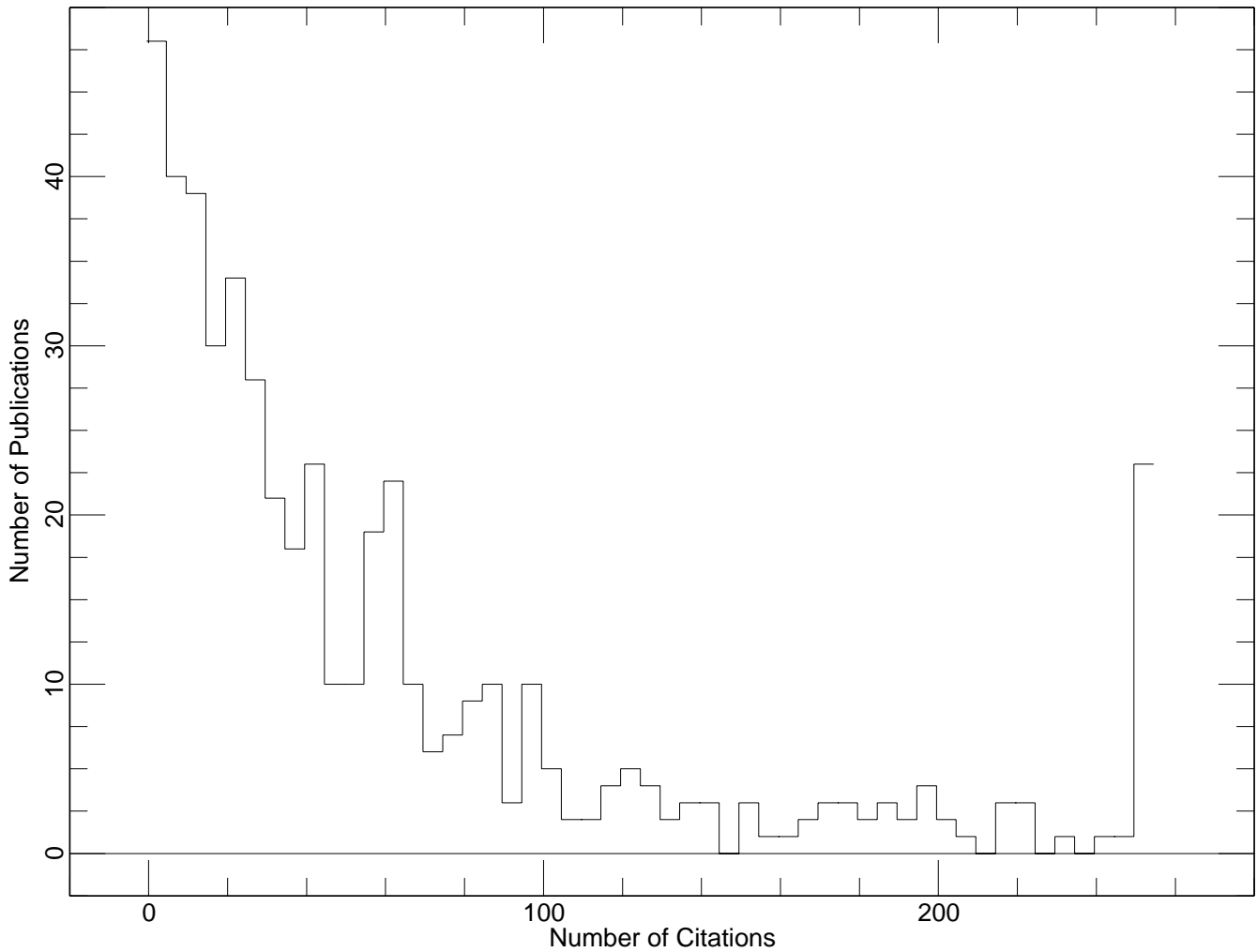
(25) The S2 Stream: The Shreds of a Primitive Dwarf Galaxy. Aguado, D., et al. 2021, MNRAS

(24) The HETDEX Instrumentation: Hobby Eberly Telescope Wide-field Upgrade and VIRUS. Hill, G., et al. 2021, AJ

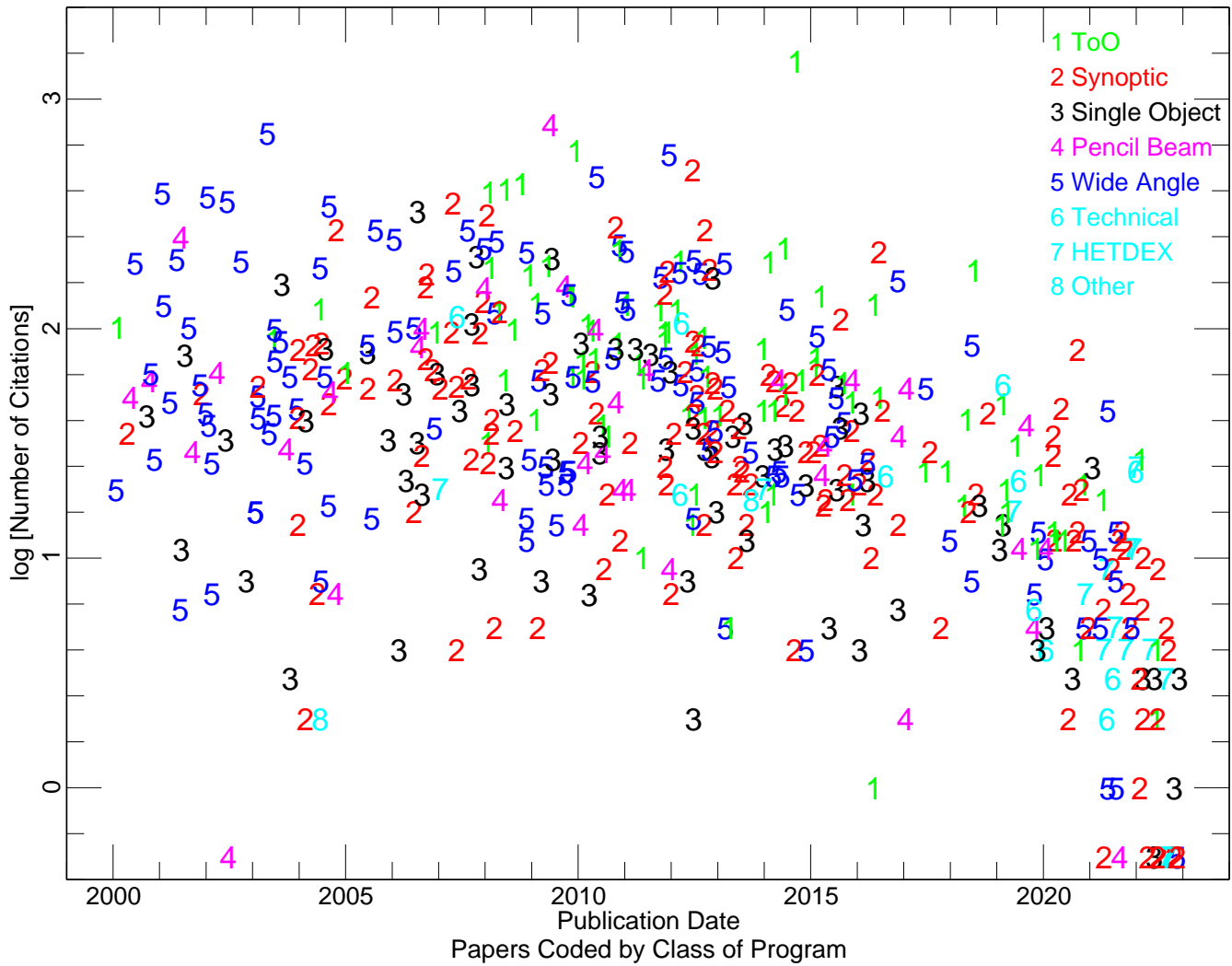
(21) The Young and Nearby Normal Type Ia Supernova 2018gv: UV-optical Observations and the Earliest Spectropolarimetry. Yang, Y., et al. 2020, ApJ



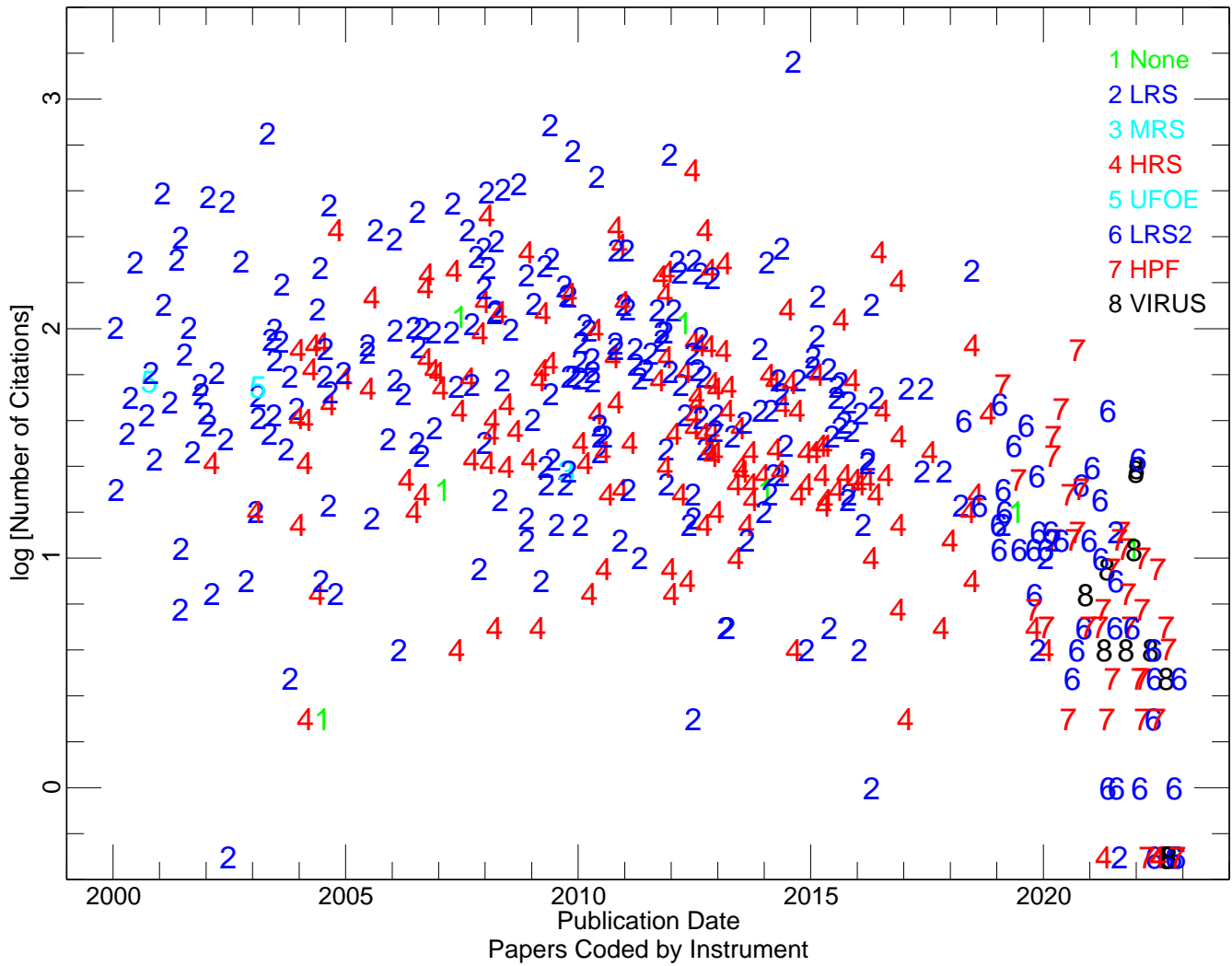
The number of HET publications each year (histogram) and the cumulative annual average of the annual number of publications (plus signs). A total of 486 HET papers have been published since the appearance of the first work in January 2000. Twenty-nine papers appeared in 2021; 28 have been published in 2021 to date.



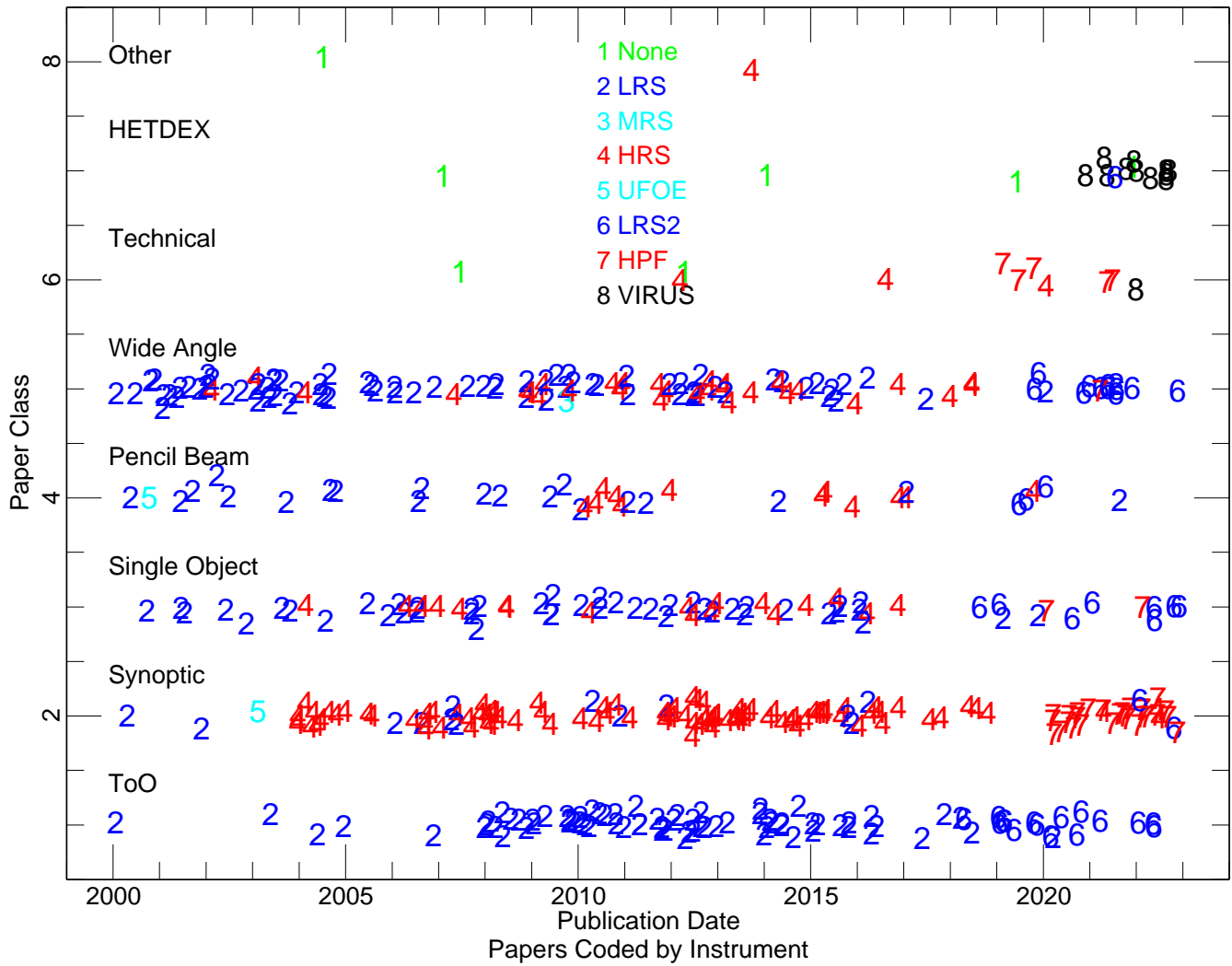
The histogram of the citation distribution of the 486 HET publications. Each bin has a width of five (e.g., the leftmost bin indicates the number of papers with 0, 1, 2, 3, or 4 citations). The rightmost bin contains all publications that have at least 250 citations (a total of 23 papers).



The logarithm of the number of citations as a function of publication date for the HET papers. (If a paper has zero citations, it is assigned a value of -0.3 .) The individual points are coded by the type of program. Most of the high-impact papers over the past decade have depended upon HET’s queue-scheduling ability (Target of Opportunity and Synoptic projects).



Identical format of the previous figure, except that the individual points are coded by the instrument used for the observations. Papers indicated by a green “1” did not use any HET observations, but were based on HET properties (e.g., the review of the HET queue operation).



The dates of publication of HET papers sorted by project class. The points are coded by instrument. The increasing importance of Target of Opportunity (primarily supernovae and gamma-ray bursts) and Synoptic (primarily exoplanets) is readily apparent in the diagram.

HET Papers Sorted by Number of Citations (November 2022)

| N | Pub | Year | Cite | Title |
|----|-----|------|------|---|
| 1 | 315 | 2014 | 1456 | Improved Cosmological Constraints From a Joint Analysis of the SDSS-III and |
| 2 | 159 | 2009 | 769 | Structure and Formation of Elliptical and Spheroidal Galaxies. |
| 3 | 38 | 2003 | 709 | A Survey of $z > 5.7$ Quasars in the Sloan Digital Sky Survey II. Discovery |
| 4 | 171 | 2009 | 597 | First-Year Sloan Digital Sky Survey-II Supernova Results: Hubble Diagram and |
| 5 | 231 | 2011 | 575 | The Second Catalog of Active Galactic Nuclei Detected by the Fermi Large Area |
| 6 | 243 | 2012 | 492 | An Abundance of Small Exoplanets Around Stars with a Wide Range of |
| 7 | 187 | 2010 | 461 | The First Catalog of Active Galactic Nuclei Detected by the Fermi Large Area |
| 8 | 141 | 2008 | 429 | Broadband Observations of the Naked-eye γ -ray Burst GRB 080319B. |
| 9 | 136 | 2008 | 403 | An Extremely Luminous X-ray Outburst at the Birth of a Supernova. |
| 10 | 123 | 2008 | 392 | The Sloan Digital Sky Survey-II Supernova Survey: Technical Summary. |
| 11 | 11 | 2001 | 391 | High-Redshift Quasars Found in Sloan Digital Sky Survey Commissioning Data IV. |
| 12 | 24 | 2002 | 375 | Towards Spectra Classification of L and T Dwarfs: Infrared and Optical |
| 13 | 29 | 2002 | 360 | Characterization of M, L, and T Dwarfs in the Sloan Digital Sky Survey. |
| 14 | 104 | 2007 | 353 | Reverberation Mapping of High-Luminosity Quasars: First Results. |
| 15 | 68 | 2004 | 344 | A Survey of $z > 5.7$ Quasars in the Sloan Digital Sky Survey. III. Discovery |
| 16 | 91 | 2006 | 325 | A Compact Supermassive Binary Black Hole System. |
| 17 | 125 | 2008 | 313 | Sodium Absorption from the Exoplanetary Atmosphere of HD 189733b Detected in |
| 18 | 197 | 2010 | 278 | The California Planet Survey. I. Four New Giant Exoplanets. |
| 19 | 111 | 2007 | 270 | The X-ray Properties of the Most Luminous Quasars from the Sloan Digital Sky |
| 20 | 70 | 2004 | 270 | Detection of a Neptune-mass Planet in the ρ^1 Cancri System Using the |
| 21 | 259 | 2012 | 269 | Kepler-47: A Transiting Circumbinary Multiplanet System. |
| 22 | 79 | 2005 | 269 | The Sloan Digital Sky Survey Quasar Catalog III. Third Data Release. |
| 23 | 16 | 2001 | 251 | The Chandra Deep Survey of the Hubble Deep Field North Area. II. Results from |
| 24 | 81 | 2006 | 246 | Binary Quasars in the Sloan Digital Sky Survey: Evidence for Excess Clustering |
| 25 | 130 | 2008 | 241 | CGRaBS: An All-Sky Survey of Gamma-Ray Blazar Candidates. |
| 26 | 202 | 2010 | 232 | Bulgeless Giant Galaxies Challenge Our Picture of Galaxy Formation by |
| 27 | 311 | 2014 | 224 | A Wolf-Rayet-like Progenitor of SN 2013cu from Spectral Observations of a |
| 28 | 119 | 2007 | 224 | Four Quasars above Redshift 6 Discovered by the Canada-France High- z |
| 29 | 198 | 2010 | 220 | The Effect of Host Galaxies on Type Ia Supernovae in the SDSS-II Supernova |
| 30 | 207 | 2011 | 219 | Supermassive Black Holes do not Correlate with Galaxy Disks or Psuedobulges. |
| 31 | 363 | 2016 | 215 | State of the Field: Extreme Precision Radial Velocities. |
| 32 | 142 | 2008 | 215 | The SEGUE Stellar Parameter Pipeline. III. Comparison with High-Resolution |
| 33 | 116 | 2007 | 206 | SN 2005ap: A Most Brilliant Explosion. |
| 34 | 160 | 2009 | 202 | Luminous Thermal Flares from Quiescent Supermassive Black Holes. |
| 35 | 13 | 2001 | 201 | Colors of 2625 Quasars at $0 < z < 5$ Measured in the Sloan Digital Sky Survey |
| 36 | 248 | 2012 | 199 | The Luminosity Function of Fermi-detected Flat-spectrum Radio Quasars. |
| 37 | 234 | 2012 | 197 | Generalized Seim-analytical Models of Supernova Light Curves. |
| 38 | 31 | 2002 | 197 | Large-Amplitude X-Ray Outbursts from Galactic Nuclei: A Systematic |
| 39 | 300 | 2014 | 195 | A Panchromatic View of the Restless SN 2009ip Reveals the Explosive Ejection of |
| 40 | 5 | 2000 | 194 | The Missing Link: Early Methane ("T") Dwarfs in the Sloan Digital Sky Survey. |
| 41 | 277 | 2013 | 193 | Oxygen Abundances in Nearby FGK Stars and the Galactic Chemical Evolution of |
| 42 | 155 | 2009 | 187 | SN 2005cs in M51 II. Complete Evolution in the Optical and the Near-Infrared. |
| 43 | 124 | 2008 | 185 | The Sloan Digital Sky Survey-II Supernova Survey: Search Algorithm and |
| 44 | 60 | 2004 | 185 | The Munich Near-Infrared Cluster Survey (MUNICS). VI. The Stellar Masses |
| 45 | 266 | 2012 | 181 | The Neptune-sized Circumbinary Planet Kepler-38b. |
| 46 | 106 | 2007 | 180 | Oxygen Abundances in Nearby Stars. Clues to the Formation and Evolution |
| 47 | 381 | 2018 | 179 | The Data Release of the Sloan Digital Sky Survey-II Supernova Survey. |
| 48 | 227 | 2011 | 177 | KOI-54: The Kepler Discovery of Tidally-Excited Pulsations and |
| 49 | 237 | 2012 | 176 | Spectroscopy of Broad-line Blazars from 1LAC. |
| 50 | 258 | 2012 | 174 | A Large Systematic Search for Close Supermassive Binary and Rapidly Recoiling |

HET Papers Sorted by Number of Citations (continued)

| N | Pub | Year | Cite | Title |
|-----|-----|------|------|--|
| 51 | 97 | 2006 | 173 | Exploring the frequency of Close-in Jovian Planets Around M Dwarfs. |
| 52 | 143 | 2008 | 171 | The Sloan Digital Sky Survey-II Photometry and Supernova Ia Light Curves |
| 53 | 220 | 2011 | 169 | The Distribution of the Elements in the Galactic Disk. III. A |
| 54 | 270 | 2012 | 167 | An Over-massive Black Hole in the Compact Lenticular Galaxy NGC 1277. |
| 55 | 367 | 2016 | 162 | The Solar Neighborhood. XXXVII: The Mass-Luminosity Relation for Main-sequence |
| 56 | 44 | 2003 | 156 | Accretion Disk Wind in the AGN Broad Line Region: Spectroscopically Resolved |
| 57 | 165 | 2009 | 154 | An Infrared/X-ray Survey for New Members of the Taurus Star-Forming Region. |
| 58 | 96 | 2006 | 152 | A Transiting Planet of a Sun-like Star. |
| 59 | 121 | 2007 | 151 | Dynamical Modelling of Luminous and Dark Matter in 17 Coma Early-Type Galaxies. |
| 60 | 225 | 2011 | 143 | The hot-Jupiter Kepler-17b: Discovery, Obliquity from Stroboscopic |
| 61 | 170 | 2009 | 142 | Rotational Velocities for M Dwarfs. |
| 62 | 164 | 2009 | 140 | Variable Sodium Absorption in a Low-extinction Type Ia Supernova. |
| 63 | 326 | 2015 | 139 | Early-time Light Curves of Type Ib/c Supernovae from the SDSS-II Supernova |
| 64 | 167 | 2009 | 139 | First-Year Sloan Digital Sky Survey-II (SDSS-II) Supernova Results: |
| 65 | 78 | 2005 | 137 | A Giant Planet Around the Massive Giant Star HD 13189. |
| 66 | 205 | 2010 | 131 | Extremely Metal-poor Stars in Classical Dwarf Spheroidal Galaxies: Fornax, |
| 67 | 120 | 2007 | 131 | XO-2b: Transiting Hot Jupiter in a Metal-rich Common Proper Motion |
| 68 | 148 | 2009 | 129 | Discovery of the Ultra-Bright Type II-L Supernova 2008es. |
| 69 | 360 | 2016 | 127 | SN 2012cg: Evidence for Interaction Between a Normal Type Ia Supernova and a |
| 70 | 204 | 2010 | 127 | Results from the Supernova Photometric Classification Challenge. |
| 71 | 10 | 2001 | 127 | High-Redshift Quasars Found in Sloan Digital Sky Survey Commissioning Data III. |
| 72 | 313 | 2014 | 122 | Binarity in Carbon-enhanced Metal-poor Stars. |
| 73 | 206 | 2011 | 122 | Supermassive Black Holes do not Correlate with Dark Matter Haloes of Galaxies. |
| 74 | 58 | 2004 | 122 | SN 2003du: Signatures of the Circumstellar Environment in a Normal Type Ia |
| 75 | 232 | 2012 | 121 | Very Early Ultraviolet and Optical Observations of the Type Ia |
| 76 | 216 | 2011 | 121 | Photometric Type Ia Supernova Candidates from the Three-Year SDSS-II SN |
| 77 | 132 | 2008 | 119 | Using Quantitative Spectroscopic Analysis to Determine the Properties and |
| 78 | 133 | 2008 | 118 | XO-3b: A Massive Planet in an Eccentric Orbit Transiting an F5 V Star. |
| 79 | 152 | 2009 | 117 | On the Magnetic Topology of Partially and Fully Convective Stars. |
| 80 | 131 | 2008 | 117 | Quasar Broad Absorption Line Variability on Multiyear Timescales. |
| 81 | 109 | 2007 | 113 | Ten Year Review of Queue Scheduling of the Hobby-Eberly Telescope. |
| 82 | 341 | 2015 | 110 | Kepler 453b - The 10 th Kepler Transiting Circumbinary Planet. |
| 83 | 238 | 2012 | 106 | Demonstration of On-sky Calibration of Astronomical Spectra Using a 25 GHz |
| 84 | 114 | 2007 | 105 | SN 2006hp: Probing the Shock Breakout of a Type II-P Supernova. |
| 85 | 178 | 2010 | 104 | First-year Sloan Digital Sky Survey-II Supernova Results: Consistency and |
| 86 | 87 | 2006 | 101 | Chandra Observations of the Highest Redshift Quasars from the Sloan |
| 87 | 18 | 2001 | 101 | High-Redshift Quasars Found in Sloan Digital Sky Survey Commissioning Data VI. |
| 88 | 2 | 2000 | 101 | GRB 991216 Joins the Jet Set: Discovery and Monitoring of Its Optical Afterglow. |
| 89 | 93 | 2006 | 100 | A Survey for New Members of Taurus with the Spitzer Space Telescope. |
| 90 | 186 | 2010 | 99 | Abundances of Red Giants in Old Open Clusters. V. Be 31, Be 32, Be 39, M 67, |
| 91 | 139 | 2008 | 99 | A Measurement of the Rate of Type Ia Supernovae at Redshift $z \sim 0.1$ from |
| 92 | 42 | 2003 | 99 | The Gamma-Ray Blazar Content of the Northern Sky. |
| 93 | 181 | 2010 | 98 | The Rise and Fall of Type Ia Supernova Light Curves in the SDSS-II Supernova |
| 94 | 82 | 2006 | 98 | Cool White Dwarfs in the Sloan Digital Sky Survey. |
| 95 | 221 | 2011 | 97 | The Effect of Peculiar Velocities on Supernova Cosmology. |
| 96 | 219 | 2011 | 97 | Improved Constraints on Type Ia Supernova Host Galaxy Properties Using |
| 97 | 105 | 2007 | 97 | Long-term Profile Variability of Double-Peaked Emission Lines in Active |
| 98 | 99 | 2006 | 97 | Multiwavelength Observations of GRB 050810A: An Exceptionally Energetic Event |
| 99 | 118 | 2007 | 96 | A Planetary-Mass Companion to the K0 Giant HD 17092. |
| 100 | 327 | 2015 | 93 | Composite Bulges: The Coexistence of Classical Bulges and Discy Psuedo-bulges |

HET Papers Sorted by Number of Citations (continued)

| N | Pub | Year | Cite | Title |
|-----|-----|------|------|---|
| 101 | 256 | 2012 | 91 | The SDSS-II Supernova Survey: Parameterizing the Type Ia Supernova Rate as |
| 102 | 39 | 2003 | 90 | GRB021004: a Massive Progenitor Star Surrounded by Shells. |
| 103 | 218 | 2011 | 89 | A More General Model for the Intrinsic Scatter in Type Ia Supernova Distance |
| 104 | 247 | 2012 | 88 | A Detection of H α in an Exoplanetary Exosphere. |
| 105 | 45 | 2003 | 88 | The Chandra Deep Field North Survey. XV. Optically Bright, X-ray-Faint Sources. |
| 106 | 174 | 2010 | 87 | The Old and Heavy Bulge of M31 I. Kinematics and Stellar Populations. |
| 107 | 199 | 2010 | 86 | Single or Double Degenerate Progenitors? Searching for Shock Emission in the |
| 108 | 61 | 2004 | 86 | Searching for Planets in the Hyades. V. Limits on Planet Detection in the |
| 109 | 383 | 2018 | 85 | CARMENES Input Catalog of M Dwarfs. III. Rotation and Activity from High |
| 110 | 255 | 2012 | 85 | The PTF Orion Project: A Possible Planet Transiting a T-Tauri Star. |
| 111 | 76 | 2005 | 85 | A Northern Survey of Gamma-Ray Blazar Candidates. |
| 112 | 57 | 2004 | 85 | Dynamical Mass Constraints on Low-Mass Pre-Main-Sequence Stellar Evolutionary |
| 113 | 264 | 2012 | 84 | Oxygen Abundances in Low- and High- α Field Halo Stars and the |
| 114 | 89 | 2006 | 83 | The Spatial Distribution of Brown Dwarfs in Taurus. |
| 115 | 295 | 2013 | 82 | The Very Young Type Ia Supernova 2013dy: Discovery, and Strong Carbon |
| 116 | 211 | 2011 | 82 | Implications of Dramatic Broad Absorption Line Variability in the Quasar |
| 117 | 200 | 2010 | 82 | A Tidal Disruption Flare in Abell 1689 from an Archival X-ray Survey of Galaxy |
| 118 | 65 | 2004 | 82 | Q0906+6930: The Highest Redshift Blazar. |
| 119 | 421 | 2020 | 81 | A Giant Planet Candidate Transiting a White Dwarf. |
| 120 | 50 | 2003 | 81 | A Dedicated M-Dwarf Planet Search Using The Hobby-Eberly Telescope. |
| 121 | 276 | 2013 | 80 | H α Activity of Old M Dwarfs: Stellar Cycles and Mean |
| 122 | 74 | 2005 | 79 | X-Ray Lighthouses of the High-Redshift Universe. II. Further Snapshot |
| 123 | 249 | 2012 | 78 | Linking Type Ia Supernova Progenitors and Their Resulting Explosions. |
| 124 | 215 | 2011 | 78 | A Population of X-Ray Weak Quasars: PHL 1811 Analogs at High Redshift. |
| 125 | 17 | 2001 | 77 | Hubble Space Telescope Images of Stephan's Quintet: Star Cluster Formation in a |
| 126 | 323 | 2015 | 75 | A Luminous, Fast Rising UV-transient Discovered by ROTSE: A Tidal Disruption |
| 127 | 224 | 2011 | 75 | The Chemical Abundances of Stars in the Halo (CASH) |
| 128 | 195 | 2010 | 75 | Hot Subdwarf Stars in Close-up View. II. Rotational Properties and Wide |
| 129 | 184 | 2010 | 74 | Measurements of the Rate of Type Ia Supernovae at Redshift ~ 0.3 from |
| 130 | 95 | 2006 | 74 | The First Extrasolar Planet Discovered with a New-Generation High-Throughput |
| 131 | 43 | 2003 | 73 | Chandra and XMM Newton Observations of the First Quasars: X-Rays From the Age |
| 132 | 173 | 2010 | 72 | Early- and Late-Time Observations of SN 2008ha: Additional Constraints for the |
| 133 | 158 | 2009 | 71 | A Search for Multi-Planet Systems Using the Hobby-Eberly Telescope. |
| 134 | 210 | 2011 | 70 | SN 2008 am: A Super-luminous Type II _n Supernova. |
| 135 | 324 | 2015 | 68 | The Broad-lined Type Ic SN 2012ap and the Nature of Relativistic Supernovae |
| 136 | 335 | 2015 | 67 | Hunting for Supermassive Black Holes in Nearby Galaxies with the Hobby-Eberly |
| 137 | 56 | 2004 | 67 | Searching for Planets in the Hyades III. The Quest for Short-Period Planets. |
| 138 | 252 | 2012 | 66 | Kinematic Signatures of Bulges Correlate with Bulge Morphologies and |
| 139 | 214 | 2011 | 66 | A Spectroscopic and Photometric Survey of Novae in M31. |
| 140 | 151 | 2009 | 66 | A Planet in a 0.6 AU Orbit Around the K0 Giant HD 102272. |
| 141 | 98 | 2006 | 66 | 2MASS J05162881+2607387: A New Low-mass Double-lined Eclipsing Binary. |
| 142 | 239 | 2012 | 65 | The McDonald Observatory Planet Search: New Long-period Giant Planets |
| 143 | 230 | 2011 | 65 | The Orbit and Companion of Probable Gamma-Ray Pulsar J2339–0533. |
| 144 | 182 | 2010 | 65 | Long-Term Profile Variability in Active Galactic Nuclei with Double-Peaked |
| 145 | 101 | 2006 | 64 | Metallicities of M Dwarf Planet Hosts from Spectral Synthesis. |
| 146 | 73 | 2004 | 64 | Signature of Electron Capture in Iron-rich Ejecta of SN 2003du. |
| 147 | 27 | 2002 | 64 | The Chandra Deep Field North Survey. IX. Extended X-Ray Sources. |
| 148 | 8 | 2000 | 64 | Five High-Redshift Quasars Discovered in Commissioning Imaging Data of the |
| 149 | 328 | 2015 | 63 | Radial Velocity Observations and Light Curve Noise Modeling Confirm that |
| 150 | 299 | 2014 | 63 | Three Planetary Companions Around M67 Stars. |

HET Papers Sorted by Number of Citations (continued)

| N | Pub | Year | Cite | Title |
|-----|-----|------|------|---|
| 151 | 260 | 2012 | 62 | The Very Young Type-Ia SN 2012cg: Discovery and Pre-Maximum Brightness |
| 152 | 172 | 2009 | 62 | Planetary Nebulae in Face-On Spiral Galaxies. III. Planetary Nebula |
| 153 | 168 | 2009 | 62 | Multi-Wavelength Properties of the Type IIB SN 2008ax. |
| 154 | 64 | 2004 | 62 | Blazar Counterparts for 3EG Sources at $-40^\circ < \delta < 0^\circ$: Pushing |
| 155 | 47 | 2003 | 62 | The Munich Near-Infrared Cluster Survey. II. The K-Band Luminosity Function |
| 156 | 213 | 2011 | 61 | PTF 10fqs: A Luminous Red Nova in the Spiral Galaxy Messier 99. |
| 157 | 177 | 2010 | 61 | Type II-P Supernovae from the SDSS-II Supernova Survey and the Standardized |
| 158 | 112 | 2007 | 61 | The Mass of the Candidate Exoplanet Companion to HD 33636 from Hubble Space |
| 159 | 72 | 2004 | 61 | High-Resolution Spectroscopy of the Transiting Planet Host Star TrES-1. |
| 160 | 349 | 2015 | 60 | The Early Days of the Sculptor Dwarf Galaxy. |
| 161 | 317 | 2014 | 60 | The Core Collapse Supernova Rate From the SDSS-II Supernova Survey. |
| 162 | 306 | 2014 | 60 | A WISE Survey of Circumstellar Disks in Taurus |
| 163 | 217 | 2011 | 60 | Silicon and Oxygen Abundances in Planet-host Stars. |
| 164 | 150 | 2009 | 60 | Calibrating M-dwarf Metallicities Using Molecular Indices: Extension to |
| 165 | 135 | 2008 | 60 | First-Year Spectroscopy for the Sloan Digital Sky Survey-II Supernova Survey. |
| 166 | 83 | 2006 | 60 | SN 2005cg: Explosion Physics and Circumstellar Interaction of Normal |
| 167 | 303 | 2014 | 59 | KIC 3858884: A Hybrid δ Scuti Pulsator in a Highly Eccentric |
| 168 | 183 | 2010 | 59 | The Evolution of Quasar C IV and Si IV Broad Absorption Lines Over |
| 169 | 7 | 2000 | 59 | Spectroscopy of Blue Stragglers and Turnoff Stars in M67 (NGC 2682). |
| 170 | 340 | 2015 | 58 | High-velocity Features of Calcium and Silicon in the Spectra of Type Ia |
| 171 | 314 | 2014 | 58 | A Misaligned Prograde Orbit for Kepler-13 AB via Doppler Tomography. |
| 172 | 267 | 2012 | 58 | Revisiting ρ^1 Cancri e: A New Mass Determination of the |
| 173 | 392 | 2019 | 57 | Stellar Spectroscopy in the Near-infrared with a Laser Frequency Comb. |
| 174 | 236 | 2012 | 57 | X-Ray and Multiwavelength Insights into the Nature of Weak Emission-line |
| 175 | 113 | 2007 | 57 | SN 2005hj: Evidence for Two Classes of Normal-Bright SNe Ia and Implications |
| 176 | 21 | 2001 | 57 | Exploratory Chandra Observations of the Highest-Redshift Quasars: X-rays from |
| 177 | 337 | 2015 | 56 | Structure and Formation of cD Galaxies: NGC 6166 in Abell 2199. |
| 178 | 281 | 2013 | 56 | Lithium-rich Field Giants in the Sloan Digital Sky Survey. |
| 179 | 108 | 2007 | 56 | Results of Monitoring the Dramatically Variable C IV Mini-BAL System |
| 180 | 36 | 2003 | 56 | The Blue Straggeler RS Canum Venaticorum Star S1082 in M67: A Detailed |
| 181 | 371 | 2017 | 55 | A Survey for New Members of the Taurus Star-forming Region with the Sloan |
| 182 | 373 | 2017 | 55 | A Large Systematic Search for Close Supermassive Binary and Rapidly |
| 183 | 273 | 2012 | 55 | The Discovery of HD 37605c and a Dispositive Null Detection of Transits of |
| 184 | 102 | 2007 | 55 | Long-Period Objects in the Extrasolar Planetary Systems 47 UMa and 14 Her. |
| 185 | 75 | 2005 | 55 | A New Detached M Dwarf Eclipsing Binary. |
| 186 | 69 | 2004 | 53 | The Chandra Deep Field-North Survey. XVII. Evolution of Magnetic Activity |
| 187 | 310 | 2014 | 52 | Hubble Space Telescope and Ground-based Observations of the Type Iax |
| 188 | 157 | 2009 | 52 | Comment on the Black Hole Recoil Candidate Quasar SDSSJ092712.65+294344.0. |
| 189 | 85 | 2006 | 52 | 51 Eridani and GJ 3305: A 10-15 Myr old Binary Star System at 30 Parsecs. |
| 190 | 20 | 2001 | 52 | Short-term Emission Line and Continuum Variations in Mrk 110. |
| 191 | 253 | 2012 | 51 | BD +48 740 – Li Overabundant Giant Star with a Planet: A Case of Recent |
| 192 | 35 | 2003 | 51 | X-Ray Lighthouses of the High-Redshift Universe: Probing the Most Luminous |
| 193 | 339 | 2015 | 50 | Massive Relic Galaxies Challenge the Co-evolution of Super-massive Black Holes |
| 194 | 362 | 2016 | 50 | Extensive Spectroscopy and Photometry of the Type IIP Supernova 2013ej. |
| 195 | 4 | 2000 | 50 | Observations of Faint, Hard-Band X-ray Sources in the Field of |
| 196 | 346 | 2015 | 48 | 500 Days of NS 2013dy: Spectra and Photometry from the Ultraviolet to the |
| 197 | 254 | 2012 | 48 | Hot Subdwarf Stars in Close-up View. II. Rotational Properties and Wide |
| 198 | 196 | 2010 | 48 | A Search for Interstellar Anthracene Towards the Perseus Anomalous Microwave |
| 199 | 12 | 2001 | 48 | High-Redshift Quasars Found in Sloan Digital Sky Survey Commissioning Data V. |
| 200 | 388 | 2019 | 47 | Photometric and Spectroscopic Properties of Type Ia Supernova 2018oh |

HET Papers Sorted by Number of Citations (continued)

| N | Pub | Year | Cite | Title |
|-----|-----|------|------|---|
| 201 | 138 | 2008 | 47 | The Hobby-Eberly Telescope Chemical Abundances of Stars in the Halo (CASH) |
| 202 | 66 | 2004 | 47 | The First Hobby-Eberly Telescope Planet: A Companion to HD 37605. |
| 203 | 308 | 2014 | 46 | WTS-2 b: A Hot Jupiter Orbiting Near its Tidal Destruction |
| 204 | 415 | 2020 | 45 | Evidence for He I 10830 Å Absorption during the Transit of a Warm Neptune |
| 205 | 49 | 2003 | 45 | Spin Orientation of Supermassive Black Holes in Active Galaxies. |
| 206 | 438 | 2021 | 44 | I Spy Transits and Pulsations: Empirical Variability in White Dwarfs Using |
| 207 | 364 | 2016 | 44 | Search for Giant Planets in M67. III. Excess of Hot Jupiters in Dense Open |
| 208 | 319 | 2014 | 44 | The Penn State - Torun' Centre for Astronomy Planet Search Stars. II. |
| 209 | 301 | 2014 | 44 | Type IIb Supernova SN 2011dh: Spectra and Photometry from the Ultraviolet to |
| 210 | 294 | 2013 | 44 | High-velocity Line Forming Regions in the Type Ia Supernova 2009ig. |
| 211 | 280 | 2013 | 44 | NLTT 5306: The Shortest Period Detached White Dwarf+Brown Dwarf Binary. |
| 212 | 110 | 2007 | 44 | The Masses and Evolutionary State of the Stars in the Dwarf Nova SS Cygni. |
| 213 | 386 | 2018 | 43 | Hydrogen and Sodium Absorption in the Optical Transmission Spectrum of |
| 214 | 353 | 2016 | 43 | A $5 \times 10^9 M_{\odot}$ Black Hole in NGC 1277 from Adaptive |
| 215 | 185 | 2010 | 43 | The Mass of HD 38529c from Hubble Space Telescope Astrometry and High-Precision |
| 216 | 22 | 2001 | 43 | The Munich Near-Infrared Cluster Survey: Number Density Evolution of Massive |
| 217 | 275 | 2012 | 42 | Testing Supernovae Ia Distance Measurement Methods with SN 2011 fe. |
| 218 | 246 | 2012 | 42 | The SDSS-HET Survey of Kepler Eclipsing Binaries: Spectroscopic Dynamical |
| 219 | 240 | 2012 | 42 | Improved Distance Determination to M51 from Supernovae 2011dh and 2005cs. |
| 220 | 41 | 2003 | 42 | The Munich Near-Infrared Cluster Survey. V. The Evolution of the Rest-frame |
| 221 | 6 | 2000 | 42 | Search for the Identification of 3EG 1835+5918: Evidence for a New Type of |
| 222 | 257 | 2012 | 41 | Type Ia Supernova Properties as a Function of the Distance to the Host Galaxy |
| 223 | 52 | 2003 | 41 | Rotational Modulation of the Photospheric and Chromospheric Activity in the |
| 224 | 37 | 2003 | 41 | Redshifts of Candidate Gamma-Ray Blazars. |
| 225 | 379 | 2018 | 40 | Breaking the Habit: The Peculiar 2016 Eruption of the Unique Recurrent Nova |
| 226 | 147 | 2009 | 40 | M31N 2007–11d: A Slowly Rising, Luminous Nova in M31. |
| 227 | 127 | 2008 | 40 | An $m \sin i = 24 M_{\oplus}$ Planetary Companion to the Nearby M Dwarf |
| 228 | 55 | 2004 | 40 | Oxygen in Open Cluster Dwarfs: Pleiades and M34. |
| 229 | 343 | 2015 | 39 | MRK 1216 and NGC 1277 - An Orbit-based |
| 230 | 288 | 2013 | 39 | Bottom-heavy Initial Mass Function in a Nearby Compact L* Galaxy. |
| 231 | 398 | 2019 | 38 | A Survey for New Members of Taurus from Stellar to Planetary Masses. |
| 232 | 188 | 2010 | 38 | A Measurement of the Rate of Type Ia Supernovae in Galaxy Clusters from the |
| 233 | 23 | 2002 | 38 | L Dwarfs Found in Sloan Digital Sky Survey Commissioning Data II. Hobby-Eberly |
| 234 | 342 | 2015 | 37 | The Black Hole in the Compact, High-dispersion Galaxy NGC 1271. |
| 235 | 285 | 2013 | 37 | BD+15 2940 and HD 233604: Two Giants with Planets Close to the Engulfment Zone. |
| 236 | 251 | 2012 | 37 | PG 1018-047: the Longest Period Subdwarf B Binary. |
| 237 | 100 | 2006 | 37 | The Spectral Energy Distribution of the High- z Blazar Q0906+6930. |
| 238 | 348 | 2015 | 36 | A Large Systematic Search for Close Supermassive Binary and Rapidly Recoiling |
| 239 | 272 | 2012 | 36 | New M, L, and T Dwarf Companions to Nearby Stars from the Wide-field |
| 240 | 269 | 2012 | 36 | The Penn State-Torun' Centre for Astronomy Planet Search Stars. |
| 241 | 140 | 2008 | 36 | The Spin-Orbit Alignment of the HD 17156 Transiting Eccentric Planetary |
| 242 | 263 | 2012 | 35 | Search for Giant Planets in M 67. I. Overview |
| 243 | 233 | 2012 | 35 | Substellar-mass Companions to the K-giants HD 240237, BD +48 738, and HD 96127. |
| 244 | 128 | 2008 | 35 | Discovery of Par 1802 as a Low-Mass, Pre-Main-Sequence Eclipsing Binary in the |
| 245 | 40 | 2003 | 35 | Search for a Point-Source Counterpart of the Unidentified Gamma-Ray Source |
| 246 | 3 | 2000 | 35 | HS 0907+1902: A New 4.2 hour Eclipsing Dwarf Novae. |
| 247 | 412 | 2020 | 34 | A Sub-Neptune-sized Planet Transiting the M2.5 Dwarf G 9-40: Validation with |
| 248 | 369 | 2016 | 34 | The Age and Distance of the Kepler Open Cluster NGC 6811 from an Eclipsing |
| 249 | 336 | 2015 | 34 | Dozens of Compact and High Velocity-dispersion, Early-type Galaxies in the |
| 250 | 282 | 2013 | 34 | The Ionized Absorber and Nuclear Environment of IRAS 13349+2438: |

HET Papers Sorted by Number of Citations (continued)

| N | Pub | Year | Cite | Title |
|-----|-----|------|------|---|
| 251 | 190 | 2010 | 34 | Radially Extended Kinematics and Stellar Populations of the Massive Ellipticals |
| 252 | 193 | 2010 | 34 | Photometric Estimates of Redshifts and Distance Moduli for Type Ia Supernovae. |
| 253 | 80 | 2005 | 33 | Variation in the Scattering Shroud Surrounding Markarian 231. |
| 254 | 28 | 2002 | 33 | Geometry and Kinematics in the Central Broad-Line Region of a Seyfert 1 Galaxy. |
| 255 | 209 | 2011 | 32 | MARVELS-1b: A Short-period, Brown Dwarf Desert Candidate from the SDSS-III |
| 256 | 175 | 2010 | 32 | The Mass of the Candidate Exoplanet Companion to HD 136118 from Hubble |
| 257 | 122 | 2007 | 32 | Constraints on Circumstellar Material Around the Type Ia Supernova 2007af. |
| 258 | 90 | 2006 | 32 | Discovery of an Extreme MeV Blazar with the SWIFT Burst Alert Telescope. |
| 259 | 394 | 2019 | 31 | The Type II-P Supernova 2017eaw: From Explosion to the Nebular Phase. |
| 260 | 332 | 2015 | 31 | Integrated Light Chemical Tagging Analyses of Seven M31 Outer Halo Globular |
| 261 | 329 | 2015 | 31 | Stellar Activity and its Implications for Exoplanet Detection on GJ 176. |
| 262 | 312 | 2014 | 31 | Broad-line Region Structure and Kinematics in the Radio Galaxy 3C 120. |
| 263 | 305 | 2014 | 30 | Evidence of Resonant Mode Coupling and the Relationship between Low and High |
| 264 | 265 | 2012 | 30 | A Radial Velocity Study of Composite-spectra Hot Subdwarf Stars with the |
| 265 | 262 | 2012 | 30 | Insights on the X-ray Weak Quasar Phenomenon from XMM-Newton Monitoring of |
| 266 | 223 | 2011 | 30 | Discovery of a ZZ Ceti in the Kepler Mission Field. |
| 267 | 46 | 2003 | 30 | Two 100 Mpc-scale Structures in the 3-D Distribution of Radio Galaxies and |
| 268 | 374 | 2017 | 29 | Search for Giant Planets in M67. IV. Survey Results. |
| 269 | 325 | 2015 | 29 | Tracking Advanced Planetary Systems (TAPAS) with HARPS-N. I. A Multiple |
| 270 | 321 | 2014 | 29 | Kepler-424 b: A “Lonely” Hot Jupiter that Found a Companion. |
| 271 | 292 | 2013 | 29 | Spectrum Syntheses of High-resolution Integrated Light Spectra of Galactic |
| 272 | 274 | 2012 | 29 | Kepler Studies of Low-mass Eclipsing Binaries. I. Parameters of the |
| 273 | 192 | 2010 | 29 | Fe I and Fe II Abundances of Solar-Type Dwarfs in the Pleides Open Cluster. |
| 274 | 189 | 2010 | 29 | Hobby-Eberly Telescope Observations of the Dark Halo in NGC 821. |
| 275 | 19 | 2001 | 29 | The Nature of the Red Giant Branches in the Ursa Minor and Draco Dwarf |
| 276 | 413 | 2020 | 28 | Kepler-1661 b: A Neptune-sized Kepler Transiting Circumbinary Planet Around a |
| 277 | 268 | 2012 | 28 | Relationship between Low and High Frequencies in Delta Scuti Stars: |
| 278 | 92 | 2006 | 28 | Spectral Line Variability Amplitudes in Active Galactic Nuclei. |
| 279 | 461 | 2022 | 27 | A WC/WO star Exploding Within an Expanding Carbon-Oxygen-Neon Nebula. |
| 280 | 355 | 2016 | 27 | Pan-Planets: Searching for Hot Jupiters Around Cool Dwarfs. |
| 281 | 161 | 2009 | 27 | PHL 1092 as a Transient Extreme X-ray Weak Quasar. |
| 282 | 146 | 2008 | 27 | Granulation in K-type Dwarf Stars. I. Spectroscopic Observations |
| 283 | 115 | 2007 | 27 | Dynamical and Observational Constraints on Additional Planets in Highly |
| 284 | 9 | 2000 | 27 | Discovery of a Close Pair of $z = 4.25$ Quasars from the Sloan Digital |
| 285 | 357 | 2016 | 26 | Toward Precision Supermassive Black Hole Masses Using Megamaser Disks. |
| 286 | 179 | 2010 | 26 | Li I and K I Scatter in Cool Pleides Dwarfs. |
| 287 | 126 | 2008 | 26 | Detection of a Third Planet in the HD 74156 System Using the Hobby-Eberly |
| 288 | 54 | 2004 | 26 | A Search for ${}^6\text{Li}$ in Lithium-Poor Stars with Planets. |
| 289 | 25 | 2002 | 26 | Convective Wavelength Shifts in the Spectra of Late-Type Stars. |
| 290 | 458 | 2021 | 25 | The Hobby-Eberly Telescope Dark Energy Experiment (HETDEX) Survey Design, |
| 291 | 430 | 2021 | 25 | The S2 stream: The Shreds of a Primitive Dwarf Galaxy. |
| 292 | 286 | 2013 | 25 | MARVELS-1: A Face-on Double-lined Binary Star Masquerading as a Resonant |
| 293 | 226 | 2011 | 25 | Kepler-15b: A Hot Jupiter Enriched In Heavy Elements and the First |
| 294 | 156 | 2009 | 25 | FIRST “Winged” and X-Shaped Radio Source Candidates. II. New Redshifts |
| 295 | 137 | 2008 | 25 | Trimming Down the Willman 1 dSph. |
| 296 | 457 | 2021 | 24 | The HETDEX Instrumentation: Hobby-Eberly Telescope Wide-field Upgrade and |
| 297 | 376 | 2017 | 24 | Abundance Tomography of Type Ia SN 2011ay with TARDIS. |
| 298 | 372 | 2017 | 24 | After the Fall: Late-Time Spectroscopy of Type IIP Supernovae. |
| 299 | 307 | 2014 | 24 | Discovery of Two Rare Rigidly Rotating Magnetosphere Stars in the APOGEE |
| 300 | 287 | 2013 | 24 | Two New Long-period Hot Subdwarf Binaries with Dwarf Companions. |

HET Papers Sorted by Number of Citations (continued)

| N | Pub | Year | Cite | Title |
|-----|-----|------|------|---|
| 301 | 169 | 2009 | 24 | Optical Spectroscopy of Bright Fermi LAT Blazars. |
| 302 | 166 | 2009 | 24 | Planetary Nebulae in Face-On Spiral Galaxies. II. Planetary Nebula |
| 303 | 405 | 2019 | 23 | SN 2017gmr: An Energetic Type II-P Supernova with Asymmetries. |
| 304 | 365 | 2016 | 23 | Follow-up Observations of Extremely Metal-poor Stars Identified from SDSS. |
| 305 | 344 | 2015 | 23 | Tracking Advanced Planetary Systems (TAPAS) with HARPS-N. II. Super |
| 306 | 330 | 2015 | 23 | Chemical Abundances in the Globular Clusters NGC 5024 and NGC 5466 from Optical |
| 307 | 309 | 2014 | 23 | Broad Absorption Line Variability in Radio-loud Quasars. |
| 308 | 304 | 2014 | 23 | Exploratory X-ray Monitoring of Luminous Radio-quiet Quasars at |
| 309 | 296 | 2013 | 23 | Constraints on a Second Planet in the WASP-3 System. |
| 310 | 397 | 2019 | 22 | 30 GHz Electro-optic Frequency Comb Spanning 300 THz in the Near Infrared and |
| 311 | 350 | 2015 | 22 | The Chemical Abundances of Stars in the Halo (CASH) Project. III. A New |
| 312 | 356 | 2016 | 22 | The Chemical Compositions of Very Metal-poor Stars HD 122563 and HD 140283: |
| 313 | 86 | 2006 | 22 | Chemical Composition of the Planet-harboring Star TrES-1. |
| 314 | 424 | 2020 | 21 | The Young and Nearby Normal Type Ia Supernova 2018gv: UV-optical Observations |
| 315 | 352 | 2016 | 21 | The Penn State-Torun Centre for Astronomy Planet Search Stars. |
| 316 | 320 | 2014 | 21 | Astrometry, Radial Velocity, and Photometry: The HD 128311 System Remixed with |
| 317 | 291 | 2013 | 21 | Secretly Eccentric: The Giant Planet and Activity Cycle of GJ 328. |
| 318 | 283 | 2013 | 21 | Host Star Properties and Transit Exclusion for the HD 38529 Planetary System. |
| 319 | 222 | 2011 | 21 | Reverberation Mapping of the Intermediate-Mass Nuclear Black Hole in |
| 320 | 163 | 2009 | 21 | A Chandra Survey of the X-ray Properties of Broad Absorption Line |
| 321 | 154 | 2009 | 21 | A Population of Metal-Poor Galaxies with L_* Luminosities at Intermediate |
| 322 | 425 | 2020 | 20 | The Habitable Zone Planet Finder Reveals a High Mass and Low Obliquity for the |
| 323 | 391 | 2019 | 20 | Observations of SN 2017ein Reveal Shock Breakout Emission and a Massive |
| 324 | 338 | 2015 | 20 | High Resolution Optical and NIR Spectra of HBC 722. |
| 325 | 298 | 2013 | 20 | Galaxy Redshift Surveys with Sparse Sampling. |
| 326 | 208 | 2011 | 20 | A Spitzer Survey of Novae in M31. |
| 327 | 203 | 2010 | 20 | Bright Variable Stars in NGC 6819: An Open Field Cluster in the Kepler Field. |
| 328 | 103 | 2007 | 20 | Probing Dark Energy with Baryonic Acoustic Oscillations at High Redshifts. |
| 329 | 1 | 2000 | 20 | The Low Resolution Spectrograph of the Hobby-Eberly Telescope II. Observations |
| 330 | 417 | 2020 | 19 | Persistent Starspot Signals on M Dwarfs: Multiwavelength Doppler Observations |
| 331 | 384 | 2018 | 19 | The Penn State-Torun Centre for Astronomy Planet Search Stars. IV. Dwarfs and |
| 332 | 361 | 2016 | 19 | Tracking Advanced Planetary Systems (TAPAS) with HARPS-N. IV. |
| 333 | 345 | 2015 | 19 | The Early Phases of the Type Iax Supernova SN 2011ay. |
| 334 | 318 | 2014 | 19 | Optimal Integrated Abundances for Chemical Tagging of Extragalactic Globular |
| 335 | 302 | 2014 | 19 | Interaction Between the Broad-lined Type Ic Supernova 2012ap and Carriers of |
| 336 | 250 | 2012 | 19 | On the Spectroscopic Classes of Novae in M33. |
| 337 | 235 | 2012 | 19 | A High-Resolution Atlas of Uranium-Neon in the H Band. |
| 338 | 194 | 2010 | 19 | Discovery of a Low-mass Companion to a Metal-rich F Star with the MARVELS |
| 339 | 94 | 2006 | 19 | R Coronae Borealis at the 2003 Light Minimum. |
| 340 | 433 | 2021 | 18 | The Peculiar Transient AT2018cow: A Possible Origin of a Type Ibn/IIn |
| 341 | 347 | 2015 | 18 | Constraining FeLoBAL Outflows From Absorption Line Variability. |
| 342 | 331 | 2015 | 18 | Three Red Giants With Substellar-Mass Companions. |
| 343 | 293 | 2013 | 18 | ROBOSPECT: Automated Equivalent Width Measurement. |
| 344 | 134 | 2008 | 18 | Spatially Resolved Spectroscopy of Coma Cluster Early-Type Galaxies. IV. |
| 345 | 385 | 2018 | 17 | The True Luminosities of Planetary Nebulae in M31's Bulge: Massive Central |
| 346 | 378 | 2018 | 17 | SN2012ab: a peculiar Type IIn supernova with aspherical circumstellar material |
| 347 | 333 | 2015 | 17 | The APOGEE Spectroscopic Survey of Kepler Planet Hosts: Feasibility, |
| 348 | 67 | 2004 | 17 | Spectroscopy of KISS Emission-Line Galaxy Candidates II. HET Observations. |
| 349 | 393 | 2019 | 16 | The Double-peaked Radio Light Curve of Supernova PTF11qej. |
| 350 | 395 | 2019 | 16 | Unbiased Cosmological Parameter Estimation from Emission-line Surveys |

HET Papers Sorted by Number of Citations (continued)

| N | Pub | Year | Cite | Title |
|-----|-----|------|------|--|
| 351 | 380 | 2018 | 16 | Tracking Advanced Planetary Systems (TAPAS) with HARPS-N. VI. HD 238914 and |
| 352 | 297 | 2013 | 16 | SN 2000cx and SN 2013bh: Extremely Rare, Nearly Twin Type Ia Supernovae. |
| 353 | 271 | 2012 | 16 | Modeling the Accretion Structure of AU Mon. |
| 354 | 88 | 2006 | 16 | Determination of the Orbit of the Planetary Companion to the Metal-Rich Star |
| 355 | 34 | 2003 | 16 | A Search for Cool Subdwarfs: Stellar Parameters for 134 Candidates. |
| 356 | 33 | 2003 | 16 | Spectroscopy of Low Surface Brightness Galaxies with the Hobby-Eberly Telescope. |
| 357 | 245 | 2012 | 15 | H-alpha Dots: A Catalog of Faint Emission-line Objects Discovered in |
| 358 | 145 | 2008 | 15 | A Chandra Look at Five of the Broadest Double-Peaked Balmer Line Emitters. |
| 359 | 77 | 2005 | 15 | The Color Selection of Quasars from Redshifts 5 to 10: Cloning and Discovery. |
| 360 | 389 | 2019 | 14 | A Recurrent Nova Super-remnant in the Andromeda Galaxy. |
| 361 | 390 | 2019 | 14 | Structural Analogs of the Milky Way Galaxy: Stellar Populations in the Boxy |
| 362 | 366 | 2016 | 14 | Very Low-mass Stellar and Substellar Companions to Solar-like Stars from |
| 363 | 354 | 2016 | 14 | The Massive Dark Halo of the Compact Early-type Galaxy NGC 1281. |
| 364 | 289 | 2013 | 14 | Analysis of Detached Eclipsing Binaries Near the Turnoff of the Open Cluster |
| 365 | 261 | 2012 | 14 | Planets Around the K-giants BD +20 274 and HD 219415. |
| 366 | 242 | 2012 | 14 | Early Ultraviolet Observations of a Type II In Supernova (2007pk). |
| 367 | 176 | 2010 | 14 | The TexOx-1000 Redshift Survey of Radio Sources I. The TOOT00 Region |
| 368 | 162 | 2009 | 14 | A Near-Infrared Spectroscopic Survey of Cool White Dwarfs in the Sloan |
| 369 | 51 | 2003 | 14 | S986 in M67: A Totally Eclipsing Binary at the Cluster Turnoff. |
| 370 | 444 | 2021 | 13 | Taking a Long Look: A Two-decade Reverberation Mapping Study of |
| 371 | 449 | 2021 | 13 | The Habitable-zone Planet Finder Detects a Terrestrial-mass Planet Candidate |
| 372 | 422 | 2020 | 13 | A Warm Jupiter Transiting an M Dwarf: A TESS Single-transit Event Confirmed |
| 373 | 410 | 2020 | 13 | An Extreme X-Ray Variability Event of a Weak-line Quasar. |
| 374 | 403 | 2019 | 13 | The Nature of Faint Radio Galaxies at High Redshifts. |
| 375 | 416 | 2020 | 12 | Discovery and Rapid Follow-up Observations of the Unusual Type II SN 2018ivc |
| 376 | 448 | 2021 | 12 | Stellar Activity Manifesting at a One-year Alias Explains Barnard b as a False |
| 377 | 429 | 2020 | 12 | Investigating the Growing Population of Massive Quiescent Galaxies at Cosmic |
| 378 | 419 | 2020 | 12 | TOI-1728b: The Habitable-zone Planet Finder Confirms a Warm Super-Neptune |
| 379 | 414 | 2020 | 12 | SN 2010kd: Photometric and Spectroscopic Analysis of a Slow-decaying |
| 380 | 411 | 2020 | 12 | It Takes Two Planets in Resonance to Tango around K2-146. |
| 381 | 377 | 2017 | 12 | What is the Milky Way Outer Halo Made of? High-resolution Spectroscopy of |
| 382 | 290 | 2013 | 12 | On the Hubble Space Telescope Trigonometric Parallax of the Dwarf |
| 383 | 201 | 2010 | 12 | Line Profile and Continuum Variability in the Very Broad-Line Seyfert |
| 384 | 144 | 2008 | 12 | In Search of the Largest Velocity Dispersion Galaxies. |
| 385 | 402 | 2019 | 11 | Interaction of SN Ib 2004dk with a Previously Expelled Envelope. |
| 386 | 456 | 2021 | 11 | First HETDEX Spectroscopic Determinations of Ly- α and UV Luminosity |
| 387 | 450 | 2021 | 11 | Nondetection of Helium in the Upper Atmospheres of TRAPPIST-1b, e, and f. |
| 388 | 453 | 2021 | 11 | Correcting Correlation Functions for Redshift-dependent Interloper |
| 389 | 407 | 2020 | 11 | Exploring the High-mass End of the Stellar Mass Function of Star-forming |
| 390 | 396 | 2019 | 11 | Variability of Low-ionization Broad Absorption-line Quasars Based on |
| 391 | 387 | 2019 | 11 | Broad Absorption Line Disappearance/Emergence in Multiple Ions in a Weak |
| 392 | 15 | 2001 | 11 | The Absorbers toward CSO118: Superclustering at $z \approx 3$, or an Intrinsic |
| 393 | 465 | 2022 | 10 | Dynamical Mass of the Young Substellar Companion HD 984 B. |
| 394 | 431 | 2021 | 10 | Revealing Efficient Dust Formation at Low Metallicity in Extragalactic |
| 395 | 406 | 2020 | 10 | An improved test of the Binary Black Hole Hypothesis for Quasars with |
| 396 | 358 | 2016 | 10 | Tracking Advanced Planetary Systems (TAPAS) with HARPS-N. III. HD 5583 and |
| 397 | 284 | 2013 | 10 | A Cautionary Tale: MARVELS Brown Dwarf Candidate Reveals Itself to be a |
| 398 | 212 | 2011 | 10 | Spectroscopic Determination of the Low-redshift Type Ia Supernova Rate from the |
| 399 | 474 | 2022 | 9 | The Warm Neptune GJ 3470b Has a Polar Orbit. |
| 400 | 441 | 2021 | 9 | The McDonald Accelerating Stars Survey (MASS): Discovery of a Long-period |

HET Papers Sorted by Number of Citations (continued)

| N | Pub | Year | Cite | Title |
|-----|-----|------|------|--|
| 401 | 437 | 2021 | 9 | The HETDEX Survey: The Ly- α Escape Fraction from 3D-HST |
| 402 | 228 | 2011 | 9 | Variable Stars in the Open Cluster NGC 7142. |
| 403 | 191 | 2010 | 9 | The XO Planetary Survey Project: Astrophysical False Positives. |
| 404 | 117 | 2007 | 9 | The Optical Emission Line Spectrum of Mark 110. |
| 405 | 443 | 2021 | 8 | The Shape and Scatter of the Galaxy Main Sequence for Massive Galaxies at |
| 406 | 382 | 2018 | 8 | A Spectroscopic Survey of Field Red-Horizontal-branch Stars. |
| 407 | 241 | 2012 | 8 | The $^7\text{Li}/^6\text{Li}$ Isotope Ratio near the Supernova Remnant IC 443. |
| 408 | 153 | 2009 | 8 | Suzaku Observations of the Extreme MeV Blazar SWIFT J0746.3+2548. |
| 409 | 62 | 2004 | 8 | Submillimetre Photometry of Typical High-redshift Radio Sources. |
| 410 | 32 | 2002 | 8 | The Beginning of the End: Hubble Space Telescope Images of Seyfert's Sextet. |
| 411 | 452 | 2021 | 7 | TOI-532b: The Habitable-zone Planet Finder confirms a Large Super Neptune in |
| 412 | 426 | 2020 | 7 | Cosmological 3D H I Gas Map with HETDEX Ly α Emitters and eBOSS QSOs |
| 413 | 399 | 2019 | 7 | The HETDEX Pilot Survey. VI. O III Emitters and Expectations for a Local |
| 414 | 229 | 2011 | 7 | Non-Detection of the Putative Substellar Companion to HD 149382. |
| 415 | 180 | 2010 | 7 | Gas Absorption in the KH 15D System: Further Evidence for Dust Settling in |
| 416 | 71 | 2004 | 7 | Photometric Identification of Cool White Dwarfs. |
| 417 | 59 | 2004 | 7 | Evidence of Planetesimal Infall on to the Very Young Herbig Be Star |
| 418 | 26 | 2002 | 7 | A Spectroscopic Reconnaissance of UV-Bright Stars. |
| 419 | 464 | 2022 | 6 | An Eccentric Brown Dwarf Eclipsing an M dwarf. |
| 420 | 435 | 2021 | 6 | The Epoch of Giant Planet Migration Planet Search Program. I. Near-infrared |
| 421 | 401 | 2019 | 6 | Impact of Crosshatch Patterns in H2RGs on High-Precision Radial Velocity |
| 422 | 368 | 2016 | 6 | The Detached Eclipsing Binary KV 29 and the Age of the Open Cluster M11. |
| 423 | 14 | 2001 | 6 | The Stanford Cluster Search: Scope Method, and Preliminary Results. |
| 424 | 479 | 2022 | 5 | TOI-3714 b and TOI-3629 b: Two Gas Giants Transiting M Dwarfs Confirmed with |
| 425 | 455 | 2021 | 5 | AGN and Star Formation at Cosmic Noon: Comparison of Data to Theoretical |
| 426 | 445 | 2021 | 5 | HETDEX [O III] Emitters. I. A Spectroscopically Selected Low-redshift |
| 427 | 454 | 2021 | 5 | A Search for Planetary Metastable Helium Absorption in the V1298 Tau System. |
| 428 | 432 | 2021 | 5 | Chemical Compositions of Red Giant Stars from Habitable Zone Planet Finder |
| 429 | 428 | 2020 | 5 | A Mini-Neptune and a Radius Valley Planet Orbiting the Nearby M2 Dwarf |
| 430 | 409 | 2020 | 5 | A Blue Ring Nebula from a Stellar Merger Several Thousand Years Ago. |
| 431 | 427 | 2020 | 5 | The H α Dots Survey. II. A Second List of Faint Emission-line Objects. |
| 432 | 400 | 2019 | 5 | The SDSS-HET Survey of Kepler Eclipsing Binaries. Description of the Survey |
| 433 | 375 | 2017 | 5 | Tracking Advanced Planetary Systems (TAPAS) with HARPS-N. V. A Massive Jupiter |
| 434 | 334 | 2015 | 5 | Proving Strong Magnetic Fields Near to the Central Black Hole in the Quasar |
| 435 | 279 | 2013 | 5 | The Unusually Luminous Extragalactic Nova SN 2010U. |
| 436 | 278 | 2013 | 5 | X-ray and Multiwavelength Insights into the Inner Structure of |
| 437 | 149 | 2009 | 5 | Discovery of a Low-Mass companion to the Solar-Type Star TYC 2534-698-1. |
| 438 | 129 | 2008 | 5 | A New, Bright, Short-Period Emission Line Binary in Ophiuchus. |
| 439 | 481 | 2022 | 4 | TOI-3757 b: A Low-density Gas Giant Orbiting a Solar-metallicity M Dwarf. |
| 440 | 471 | 2022 | 4 | Seven Years of SN 2014C: A Multiwavelength Synthesis of an Extraordinary |
| 441 | 467 | 2022 | 4 | Surface Brightness Profile of Lyman- α Halos out to 320 kpc in HETDEX. |
| 442 | 423 | 2020 | 4 | Comparative Spectral Analysis of the Superluminous Supernova 2019neq. |
| 443 | 451 | 2021 | 4 | Detection of Lyman Continuum from $3.0 < z < 3.5$ Galaxies in |
| 444 | 434 | 2021 | 4 | The Stars of the HETDEX Survey. I. Radial Velocities and Metal-poor Stars from |
| 445 | 404 | 2019 | 4 | Stellar Properties of KIC 8736245: An Eclipsing Binary with a Solar-type Star |
| 446 | 408 | 2020 | 4 | Calibrating Iodine Cells for Precise Radial Velocities. |
| 447 | 351 | 2016 | 4 | The Peculiar Optical-UV X-ray Spectra of the X-ray Weak Quasar PG 0043+039. |
| 448 | 322 | 2014 | 4 | Studying the Dwarf Galaxies in Nearby Groups of Galaxies: Spectroscopic and |
| 449 | 316 | 2014 | 4 | Determination of Mass and Orbital Parameters of a Low-mass Star HD213597B. |
| 450 | 107 | 2007 | 4 | Late-type Near-contact Eclipsing Binary [HH97] FS Aur-79. |

HET Papers Sorted by Number of Citations (continued)

| N | Pub | Year | Cite | Title |
|-----|-----|------|------|--|
| 451 | 84 | 2006 | 4 | SDSS J103913.70+533029.7: A Super Star Cluster in the Outskirts of a Galaxy |
| 452 | 484 | 2022 | 3 | A Transient "Changing-look" Active Galactic Nucleus Resolved on Month |
| 453 | 476 | 2022 | 3 | The Active Galactic Nuclei in the Hobby-Eberly Telescope Dark Energy |
| 454 | 469 | 2022 | 3 | A Quasar Shedding Its Dust Cocoon at Redshift 2. |
| 455 | 459 | 2022 | 3 | A Hot Mars-sized Exoplanet Transiting an M Dwarf. |
| 456 | 463 | 2022 | 3 | High-resolution Near-infrared Spectroscopy of a Flare around the Ultracool |
| 457 | 442 | 2021 | 3 | Broadband Stability of the Habitable Zone Planet Finder Fabry-Perot Etalon |
| 458 | 420 | 2020 | 3 | The Energetics of Launching the Most Powerful Jets in Quasars: A Study |
| 459 | 48 | 2003 | 3 | Low Signal-to-Noise Spectroscopy and Surface Photometry of Two Faint Galaxies |
| 460 | 472 | 2022 | 2 | TOI-1696 and TOI-2136: Constraining the Masses of Two Mini-Neptunes with the |
| 461 | 470 | 2022 | 2 | Close, Bright, and Boxy: the Superluminous SN 2018hti. |
| 462 | 462 | 2022 | 2 | Gaia 20eae: A Newly Discovered Episodically Accreting Young Star. |
| 463 | 440 | 2021 | 2 | A Harsh Test of Far-field Scrambling with the Habitable-zone Planet Finder and |
| 464 | 418 | 2020 | 2 | Following the TraCS of exoplanets with Pan-Planets: Wendelstein-1b and |
| 465 | 370 | 2017 | 2 | Parsec-scale Variations in the $^7\text{Li i}/^6\text{Li i}$ Isotope Ratio Toward IC 348 |
| 466 | 244 | 2012 | 2 | Discovery of a Wolf-Rayet Star Through Detection of Its Photometric |
| 467 | 63 | 2004 | 2 | Exact Optics IV. Small 'trumpet' Correctors for Large Spheres. |
| 468 | 53 | 2004 | 2 | A Search for Sodium Absorption from Comets Around HD209458. |
| 469 | 482 | 2022 | 1 | Understanding the Spatial Variation of Mg II and Ionizing Photon Escape in a |
| 470 | 460 | 2022 | 1 | The Great Slump: Mrk 926 Reveals Discrete and Varying Balmer Line Satellite |
| 471 | 446 | 2021 | 1 | Multiepoch Spectroscopy of Mg II Broad Absorption Line Transitions. |
| 472 | 439 | 2021 | 1 | Probing the Disk-Corona Systems and Broad-line Regions of Changing-look |
| 473 | 359 | 2016 | 1 | Possible Detection of Singly Ionized Oxygen in the Type Ia SN 2010kg. |
| 474 | 475 | 2022 | 0 | The SDSS-HET Survey of Kepler Eclipsing Binaries. A Sample of Four Benchmark |
| 475 | 486 | 2022 | 0 | The Active Chromospheres of Lithium-rich Red Giant Stars. |
| 476 | 480 | 2022 | 0 | Stellar Populations of Ly-emitting Galaxies in the HETDEX Survey. I. An |
| 477 | 483 | 2022 | 0 | Revising Properties of Planet-Host Binary Systems. II. Apparent |
| 478 | 485 | 2022 | 0 | Chemical Abundances of Eight Highly-extincted Milky Way Planetary Nebulae. |
| 479 | 478 | 2022 | 0 | $\text{Ly}\alpha$ Halos around [O III]-selected Galaxies in HETDEX. |
| 480 | 477 | 2022 | 0 | The Active Galactic Nuclei in the Hobby-Eberly Telescope Dark Energy |
| 481 | 473 | 2022 | 0 | The η Aquilae System: Radial Velocities and Astrometry in Search of |
| 482 | 466 | 2022 | 0 | Rotational Modulation of Spectroscopic Zeeman Signatures in Low-mass Stars. |
| 483 | 468 | 2022 | 0 | The Energetics of the Central Engine in the Powerful Quasar 3C 298. |
| 484 | 447 | 2021 | 0 | A Galaxy Cluster in the Innermost Zone of Avoidance, Close to the Radio |
| 485 | 436 | 2021 | 0 | Tracking Advanced Planetary Systems (TAPAS) with HARPS-N. VII. Elder Suns with |
| 486 | 30 | 2002 | 0 | Suspected Wolf-Rayet Galaxies UM 456 and UM 594. |